Characterization of the Semiconductor Optical Amplifier for Amplification and Photonic Switching Employing the Segmentation Model

Abd El Aziz[1], W. P. Ng[1], *Member, IEEE*, Z. Ghassemlooy[1], *Senior Member, IEEE* , Moustafa H. Aly[2] *Member OSA*, R. Ngah[3] and M. F. Chiang[1],
Northumbria Communications Research Laboratory
[1]*Northumbria University, Newcastle upon Tyne, UK*
Tel: (+44)1912273841, e-mail: {ahmed.shalaby, w.p.ng, fary.ghassemlooy@unn.ac.uk}
[2]*Arab Academy for Science and Technology and Maritime Transport, Alexandria, Egypt*
[3]*Universiti Teknologi, Malaysia*

***Abstract*—This paper characterizes the gain and the carrier density responses of a semiconductor optical amplifier (SOA). In order to achieve the switching functions in SOA-based optical switches, such as Symmetric Mach-Zehnder (SMZ), the effect of the input signal on the total gain response of the SOA is investigated. The theoretical operation principle is demonstrated using a segmentation model that employs the complete rate equation with third order gain coefficients. Results obtained show the input boundaries and requirements in which the SOA can be efficiently used as an amplifier and as a switch.**

Keywords: carrier density, gain response, semiconductor optical amplifier (SOA), stimulated emission.

1. INTRODUCTION

To overcome the speed bottleneck imposed by the optoelectronic conversions, ultrafast photonic networks rely on photonic signal processing. Semiconductor optical amplifier (SOA) is considered as the key component in the next generation of optical networks [1]. Not only can the SOA be used as a general gain unit but it also has many functional applications including all optical switching, wavelength conversion, and optical logic signal processing [2]. Ultrafast all-optical switches based on SOA, such as Mach-Zehnder Interferometers (MZIs) [3] are the most promising candidates for the realization of all-optical switching and processing applications compared to other all-optical switches, such as ultrafast-nonlinear interferometers (UNIs) and Terahertz Optical Asymmetric Demultiplexers (TOADs) due to their compact size, high stability, low switching energy, high integration potential and their fast and strong nonlinearity characteristics [4-6].

Moreover, the use of SOAs as in-line amplifiers is very suitable for bi-directional transmission in local and metropolitan systems and networks because of the lower cost of SOAs and no need for optical isolators as often used in different types of amplifiers such as erbium doped fiber amplifiers (EDFAs) [7].

The key characteristics of a SOA are the time evolution of the gain, carrier density and stimulation emission of an SOA following pump pulse propagation. In gain dynamics studies including pump and continuous wave (CW) probe propagation, a few models have been proposed [8, 9]. Several works have addressed the gain responses but without investigating a direct relationship to the wavelength of the signal and the applied bias current. Here, we propose a direct temporal analysis of the effect of the input signal wavelength, the applied bias current and the input power of the signal, based on a segmentation model that we have developed, which takes into account forward pump and probe propagation.

In this paper, we investigate the optimum parameters of the SOA required in order to perform amplification and switching functions. The key optimizations are achieved by controlling the bias current to the corresponding input signal power within the wavelengths. The effect of the optimization of the carrier density and the gain responses in order to control amplification and switching are investigated. The SOA amplification process and model used is explained in the following section while section 3 presents the boundary conditions and requirements for the SOA to perform amplification and switching. The final section concludes the findings of the investigation.

2. SOA AMPLIFICATION PROCESS AND THE SEGMENTATION MODEL

The process begins when a direct current (DC) is applied to the active region of the SOA, thus giving electrons in the valence band enough energy to overcome the energy gap and hence, populating the conduction and valence bands (energy levels) with electrons and holes, respectively [10]. The process which provides amplification is the stimulated emission. This process occurs when an incoming optical beam is launched into the active region of the SOA via the input facet of the amplifier; an incident photon collides with an excited electron from the conduction band releasing a stimulated photon with the same phase, frequency and direction. More identical photons are

released by the collision of the incident beam of photons with more excited electrons in the conduction band thus amplifying the input signal [10]. The reduction of excited electrons in the conduction band (i.e. drop in the carrier density) will result in a decrease of the SOA gain because the gain is proportional to the carrier population. Moreover, it will increase the active refractive index due to the nonlinear refractive index being dependent on the carrier density [11, 12].

When an input optical pulse with a short width is launched into the SOA, stimulation emission will take place resulting in signal amplification. Therefore, the carrier density will be reduced thus causing a drop in the SOA gain. The carrier non-equilibrium is governed mainly by the spectral hole burning effect [13, 14]. The distribution recovers to the equilibrium by the carrier-carrier scattering. Instantaneous mechanisms such as two-photon absorption [15, 16] and the optical Kerr effects [17, 18] will then influence on the SOA response. After few picoseconds, a quasi-equilibrium distribution due to the carrier temperature relaxation process will ensure the carrier density recovery [10].

The rate equations of SOA are iteratively calculated while taking the carrier density changes and the SOA length in account. The dynamic equation for the change in the carrier density within the active region of the device is given by:

$$\frac{dN}{dt} = \frac{I}{q \cdot V} - (A.N + B.N^2 + C.N^3) - \frac{\Gamma \cdot g \cdot P_{av} \cdot L}{V \cdot h \cdot f}, \tag{1}$$

where I is the DC current injected to the SOA, q is the electron charge and V is the active volume of the SOA, Γ is the confinement factor, P_{av} the average output power, L is the SOA length, h is the Plank constant and f is the light frequency. A is the surface and defect recombination coefficient while B and C are the radiative and Auger recombination coefficients, respectively. The gain medium of the amplifier is described by the material gain coefficient, g (per unit length), which is dependent on the carrier density N and the signal wavelength λ and is given by:

$$g = \frac{\alpha_g (N - N_0) - a_2 (\lambda - \lambda_N)^2 + a_3 (\lambda - \lambda_N)^3}{1 + \varepsilon P_{av}}, \tag{2}$$

where a_2 and a_3 are empirically determined constants that characterize the width and asymmetry of the gain profile, respectively. α_g is the differential gain parameter, N_o is the carrier density at transparency point, λ_N represents the corresponding peak gain wavelength with λ_o being the peak gain wavelength at transparency, a_4 denoting the empirical constant that shows the shift of the gain peak and ε is the gain compression factor.

$$\lambda_N = \lambda_O - a_4 (N - N_O), \tag{3}$$

The rate equations in [19] are carried out via Matlab™ to investigate the gain response of the SOA model by employing the segmentation method. This model involves dividing the SOA into five equally segments of length $l = L/5$ each were l is the segment length. The carrier density is assumed to be constant within a segment. However, the carrier density changes from one segment to another depending on its input power and the carrier density of the previous segment. The reason that five segments were chosen is to investigate the change in the carrier density along the SOA for a 1.2 ps pulse width [10].

3. RESULTS AND DISCUSSION

The physical SOA parameters used for our proposed model are given in Table 1 [20]. The normalized gain response of the SOA using the physical parameters in the table with no input signal launched into the SOA can be shown in Fig. 1. The rapid increase of the gain from time zero till reaching a steady state value where the gain becomes constant is due to the biasing of the SOA. A large number of electrons in the valence band will gain enough energy to overcome the energy gap, increasing the carrier density (number of electrons in the conduction band) and hence increasing the SOA total gain. In this simulation, we will study the response of a pump and a CW probe signals on the SOA gain in order to investigate the boundary conditions and requirements to amplify and switch input signals. The first input is a short pulse signal with a pulse width of l/v_g (i.e. 1.2 ps), where v_g is the group velocity of the signal inside the active region of the waveguide. From Fig. 2 one can observe the drop in the gain instantly when an input pulse enters the SOA. This drop in gain is because of interaction between the input signal and the excited electrons in the conduction band leading to a sudden decrease in the carrier density and therefore depletion in the SOA gain. This depletion is the signal output gain and it depends on the power and the pulse width of the input signal which we will discuss at the end of this section. After the input signal pulse has exited the active region, the gain recovers back to its steady state value.

Table 1. Physical SOA parameters.

Parameter	**Symbol**	**Value/Unit**
Carrier density at transparency	N_0	1.4×10^{24} /m^3
Wavelength at transparency	λ_o	1605 nm
Initial carrier density	N_i	3×10^{24} /m^3
Signal wavelength	λ	1550 nm
Internal waveguide scattering loss	α_s	40×10^{2} /m
Differential gain	α_g	2.78×10^{-20} m^2
Gain constant	a_2	7.4×10^{18} /m^3
Gain constant	a_3	3.155×10^{25} /m^4
Gain peak shift coefficient	a_4	3×10^{-32} m^4
SOA length	L	500 µm
SOA width	W	3 µm
SOA height	H	80 nm
Confinement factor [21]	Γ	0.3
Light frequency	f	193.5 THz
Plank constant	h	6.62606896×10^{-34}
Electron charge	q	1.602×10^{-19} C
Surface and defect recombination coefficient	A	1.43×10^{8} 1 /s
Radiative recombination coefficient	B	1×10^{-16} m^3 /s
Auger recombination coefficient	C	3×10^{-41} m^6 /s
Gain compression factor	E	0.2 /W
Bias current	I	150 mA

The second input signal applied to the SOA is the CW probe signal, which causes a continuous reduction in it's the SOA gain until reaching the saturation gain level, see Fig. 3. The reason for this response is that a depletion of the carrier density happens because of the continuous stimulation emission process. The carrier density, and hence the gain, continues to decrease until excited electrons in the conduction band are no longer available.

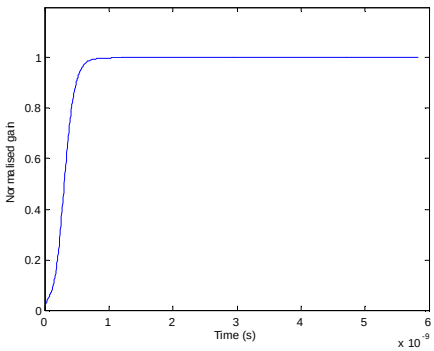

Figure. 1. Normalized gain response of the SOA.

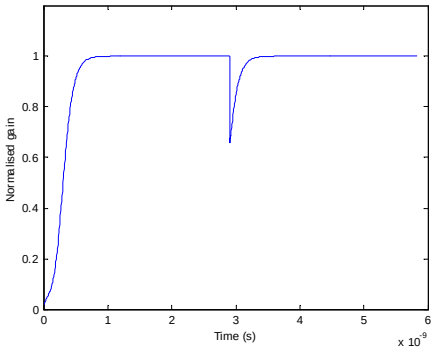

Figure. 2. Normalized gain response of the SOA due to a short input pulse.

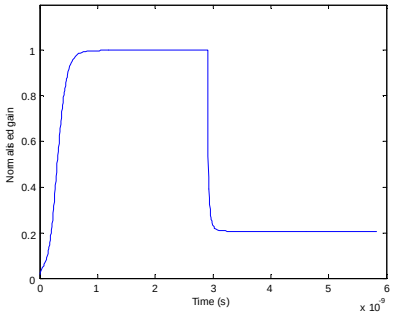

Figure. 3. Normalized gain response of the SOA due to a CW probe.

3.1 Amplification

In order to use the SOA as an amplifier, we should ensure that the signal will not be affected by the SOA nonlinear response that occur when the SOA gain reaches its saturation value as shown in Fig. 3. A range of input pulse signals with optical power values from 1 mW to 10 mW were applied to the SOA, and the signal output gains are illustrated in Fig. 4. As expected, the figure shows that the gain drops with increasing the input signal power. This effect is because signal with a signal with higher power will interact with a larger number of excited electrons in the conduction band, thus resulting in increased depletion in the carrier density and the SOA gain.

This process is repeated with a range of signals of different wavelengths within the C-band which (i.e. 1530 nm to 1565 nm). As it can be seen from Fig. 4, for input powers less than 3 mW the gain is higher for higher values of wavelength A signal with 1 mW of power at 1530 nm and 1565 nm shows gains of 102 and 138, respectively. From the shown results, for 3 mW input signal the output gain will be nearly the same regardless of the signal wavelength. The figure also illustartes variation in the rate of change of the gain difference due to different wavelengths of the input pulse. As it can be seen from Fig. 4, the lower wavelength achieves higher gain for input powers more than 3 mW.

Figure 5 displays the gain difference between the saturation gain (i.e. maximum limit for amplification) and the signal output gain for all signal powers at different wavelengths used within the C-band range. From the figure, it can be seen that the gain difference decreases when the input power increases and reaching saturation gain at input power > 10 mW. The reason for this is that the higher the input power will result in greater depletion carrier density which in turn reduces the SOA gain. For example, at 1530 nm saturation gains are 39 and 27.5 for input powers of 1 mW and 2 mW, respectively. Correspondingly, the rate of change of the gain difference response also varies due to the close saturation values. Figure 6 illustrates both the saturation gain and the signal output gain at 1550 nm and 1565 nm for an injected bias current of 180 mA. The 1550 nm was chosen because it is the most common used wavelength in all applications while 1565 nm was chosen because it achieves the best output gain within the C-band range for input powers less than 3 mW (In most applications input signal is <3 mW).

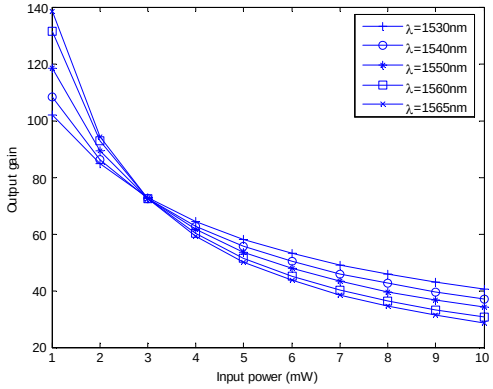

Figure. 4. Signal output gain corresponding to the input power at different wavelengths.

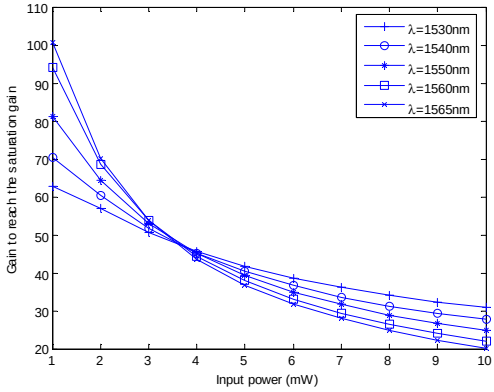

Figure. 5. Difference between the output and saturation gain corresponding to the input power at different wavelengths.

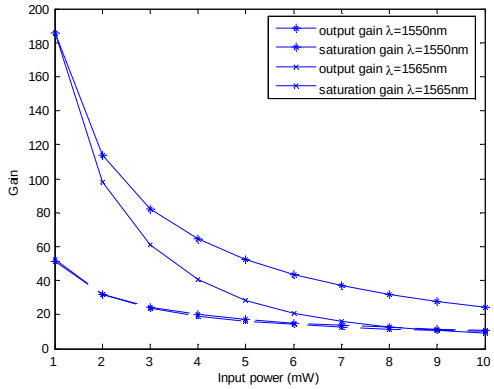

Figure. 6. Output and saturation gain corresponding to the input power at different wavelengths at I = 180 mA.

Comparing Fig. 6 with Fig. 5 (where I = 150 mA) shows the output gain is higher for higher values of bias current. Figure 6 also shows that the gain for input signals with power >8 mW at 1565 nm reaches saturation and therefore drives the SOA into nonlinearity, which is useful for switching operation.

3.2 Switching

In order to use the cross phase modulation (XPM) characteristics of SOA for switching function, ideally the signal should be affected by the nonlinearity of the SOA achieving a phase shift of 180^o for the complete deconstructive interference [22]. This phase shift can be obtained by the aid of a control pulse (CP) which is injected to the active region of the SOA in order to achieve gain depletion thus the gain saturation. When the total gain reaches the saturation level, a phase shift of 180^o will be achieved by the input signal [23]. Figure 7 illustrates the CP power against the input signal powers for a range of wavelengths. Results show that signals at lower wavelengths (i.e. 1530 nm) require higher CP power to achieve XPM in the SOA. The gain difference between signals with different wavelengths continues to increase with the input power (see Fig. 4). Thus the divergence of CP needed between different wavelengths at higher values of input power as shown in Fig. 7. Signals with low input powers have higher saturation gain and therefore requiring CPs with low power to deplete the SOA gain to achieve switching.

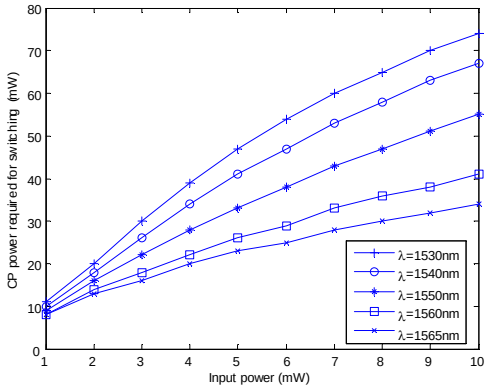

Figure 7. The CP power versus the input signal power for a range of wavelengths.

4. CONCLUSION

This paper has simulated the total gain response of an SOA model using the segmentation method. CW probe and pump signals were applied to the proposed segmentized SOA model to investigate the corresponding gain response in order to achieve amplification and all-optical switching, respectively. The optimum performance conditions regarding the input signal power, the bias current and the signal wavelengths were investigated for the SOA to function as an amplifier and a switch.

REFERENCES

[1] I. Armstrong, I. Andonovic, and A. Kelly, "High performance semiconductor optical amplifiers," *Journal of optical networking,* vol. 3, pp. 882-897, 2004.

[2] M. Connelly, *Semiconductor optical amplifiers.* New York: Springer-Verlag, 2002.

[3] S. Nakamura, K. Tajima, and Y. Sugimoto, "Experimental investigation on high-speed switching characteristics of a novel symmetric Mach-Zehnder all-optical switch," *Applied Physics Letter,* vol. 65, pp. 283-385, 1994.

[4] R. Giller, R. Manning, and D. Cotter, "Gain and phase recovery of optically excited semiconductor optical amplifiers," *IEEE photonics technology letters,* vol. 18, pp. 1061-1063, 2006.

[5] J. Moerk, M. Nielsen, and T. Berg, "The dynamics of semiconductor optical amplifiers-modeling and applications," *Optics and Photonics News,* vol. 14, pp. 42-48, 2003.

[6] E. Tangdiongga, Y. Liu, H. Waardt, G. Khoe, A. Koonen, and H. Dorren, "All-optical demultiplexing of 640 to 40 Gbits/s using filtered chirp of a semiconductor optical amplifier," *Optics Letters,* vol. 32, pp. 835-837, 2007.

[7] J. Yu, Y. Yeo, O. Akanbi, and G. Chang, "Bi-directional transmission of 8 X 10Gb/s DPSK signals over 80 km of SMF-28 fiber using in-line semiconductor optical amplifier," *Optics Express,* vol. 12, pp. 6215-6218, 2005.

[8] K. Obermann, I. Koltchanov, K. Petermann, S. Diez, R. Ludwig, and H. Weber, "Noise analysis of frequency converters utilizing semiconductor-laser amplifiers," *IEEE JOURNAL OF QUANTUM ELECTRONICS*, vol. 33, pp. 81-88, 1997.

[9] H. Soto Ortiz and D. Erasme, "Modelling and experimental measurements of the switching behaviour of semiconductor optical amplifiers " *Optical and Quantum Electronics*, vol. 28, pp. 669-682, 1996.

[10] H. Le Minh, "All-optical router with PPM header processing high speed photonic packet switching networks," PhD Thesis, Northumbria University, 2007.

[11] G. Agrawal and N. Olsson, "Self-phase modulation and spectral broadening of optical pulses in semiconductor laser amplifiers," *IEEE journal on selected topics in quantum electronics*, vol. 25, pp. 2297-2306, 1989.

[12] M. Eiselt, W. Pieper, and H. Weber, "SLALOM: Semiconductor laser amplifier in a loop mirror," *IEEE journal of lightwave technology*, vol. 13, pp. 2099-2112, 1995.

[13] L. Guo and M. Connelly, "All-optical AND gate with improved extinction ratio using signal induced nonlinearities in a bulk semiconductor optical amplifier," *optics Express*, vol. 14, pp. 2938-2943, 2006.

[14] P. Borri, W. Langein, J. Hvam, F. Heinrichsdorff, M. Mao, and D. Bimberg, "Spectral hole-burning and carrier-heating dynamics in quantum-dot amplifiers: comparison with bulk amplifiers," *physica status solidi*, vol. 224, pp. 419-423, 2001.

[15] H. Ju, A. Uskov, R. Notzel, Z. Li, J. Vazquez, D. Lenstra, G. Khoe, and H. Dorren, "Effects of two-photon absorption on carrier dynamics in Quantum-dot optical amplifiers," *applied physics B. lasers and optics*, vol. 82, pp. 615-620, 2006.

[16] K. Tajima, S. Nakamura, and Y. Ueno, "Semiconductor nonlinearities for ultrafast all-optical gating," *measurement science and technology*, vol. 13, pp. 1692-1697, 2002.

[17] G. Agrawal, *Nonlinear fiber optics*, 2 ed. San Diego, USA: Academic Press, 1995.

[18] J. Mendoza-Alvarez, L. Coldren, A. Alping, R. Yan, T. Hausken, K. Lee, and K. Pedrotti, "Analysis of depletion edge translation lightwave modulators," *IEEE journal of lightwave technology*, vol. 6, pp. 793-807, 1988.

[19] H. Wang, J. Wu, and J. Lin, "Studies on the material transparent light in semiconductor optical amplifiers," *Journal of Optics A:Pure and Applied Optics*, vol. 7, pp. 479-492, 2005.

[20] VPIsystems, *VPI transmission maker and VPI component maker: photonic modules reference manual*, 2001.

[21] F. Tabatabai and H. S. Al-Raweshidy, "Feedforward linearization technique for reducing nonlinearity in semiconductor optical amplifier " *Journal of Lightwave Technology*, vol. 25, pp. 2667-2674, 2007.

[22] M. F. Chiang, Z. Ghassemlooy, W. P. Ng, and H. Le Minh, "Simulation of an all-optical 1 x 2 SMZ switch with a high contrast ratio," *Proceeding of the 8th annual PostGraduate Symposium on the convergence of Telecommunicatios, Networking and Broadcasting (PGNET 2007)*, pp. 65-69, 2007.

[23] Z. Ghassemlooy, W. P. Ng, and H. Le Minh, "BER performance analysis of 100 and 200 Gb/s all-optical OTDM node using symmetric Mach-Zehnder switches," *IEE proceedings Circuit, Devices and Systems on Commun. Systs. Network and DSP*, vol. 153, pp. 361-369, 2006.